MOTION CORRECTION FOR FUNCTIONAL INFRARED IMAGING

A. Tangherlini*, A. Merla*,** and G.L. Romani*,**

* Department of Clinical Sciences and Bioimaging, School of Medicine, University of Chieti-Pescara, Chieti, Italy
** ITAB – Institute of Advanced Biomedical Technologies, Foundation "G. D'Annunzio University", Chieti, Italy

andytanga@hotmail.com

Abstract: Motion correction (MC) is a well-known problem in biomedical imaging. Almost all the algorithms available have been developed for fMRI and PET image series. Functional Infrared Imaging (fIRI) relies on the study of the thermoregulatory response through thermal image series to functional stimulation. No specific algorithms are currently developed for MC of fIRI image series. Here we propose a method suitable for fIRI based on rigid body transformations, the parameters of which are determined monitoring relative positions of paper land-marks put on the skin. Two methods are proposed to semi-automatically determine the position of the markers in images: One is based on the calculus of the center of gravity of coldest (hottest) points (Centre of Mass Method); the other is based on correlation properties (Correlation Based Method). Both of them are compared to human selection and to a commercial non-fIRI dedicated program, and then benchmarked. Tests demonstrate the consistency of these methods, in particular CMM is fastest but less accurate than CBM, and both of them are more accurate than the chosen non-fIRI dedicated program. Furthermore the CBM can be applied in a wider range of applications.

Introduction

MC is a well-known problem in biomedical imaging. Many studies have been performed and several algorithms have been proposed to solve the problem [1, 2], mostly dealing with MC of fMRI and PET image series [3, 4].
Recently, functional infrared imaging (fIRI) has been proposed as a novel biomedical imaging technique [5-12]. An important requirement for fIRI data processing is MC of a series of thermal images, the temperature range of which may dramatically changes along the time. Since fMRI and/or PET MC techniques do not need usually taking into account large variations of the signal intensity for a given pixel or Region of Interest (ROI), those techniques result not easily adaptable or immediately valid for fIRI.

In addition, fIRI images are 2-dimensional while fMRI and PET ones are 3-dimensional. A general feature of fMRI and PET MC algorithms is the use of minimization techniques based on the differences between images [1]. Such an approach may provide effective MC when applied to thermal image series without large temperature variations along time (e.g. psychometric studies [10]). Unfortunately, there are many other processes, like the response to thermal stress stimulation (e.g. Raynaud's phenomenon [11, 12]) or physical activity [9] where no-one of the available MC algorithms is effective. A novel fIRI-dedicated algorithm applicable to such processes is therefore hereby proposed and discussed.

Materials and Methods

The proposed correction relies on a shape-preserving mapping model [13]. Actually we need to consider that the thermal image is a 2-d projection of a 3-d body onto a plane perpendicular to the axes of the camera optics (projection plane). To limit the complexity of the problem, we allow the rigid body to move only in a plane parallel to the projection one. This allow us to reduce the MC parameters to 3 (if the body rotates in the plane) or 2 (if the body simply translates into the plane). To compute these parameters, we need to know the position of reference markers on each image of the series. We used paper markers put on the skin as a reference markers, since their temperature hardly resembles skin temperature variations.

Since each marker is associated with its 2 coordinates in the plane, it provides 2 conditions to be satisfied by each equation of the transformation. Therefore, we need to use a single marker to correct 2-d translations of the Region of Interest (ROI); and 2 markers to correct 2-d translations coupled to a plane rotation. We developed 2 different techniques to find out the position of the markers on each image of the series:

1. Centre of Mass Method (CMM), which relies on the general feature that the paper marker has usually different temperature with respect to its surrounding tissue. Thus we can define a threshold to compute and to locate the centre of gravity of the marker within a given ROI. The threshold can be manually or automatically chosen. In the latter case, an algorithm finds the coldest (hottest) temperature in the ROI and automatically set the threshold above (below) it, thus allowing to recognize the marker and track its position even for large temperature variation.

ISSN: 1727-1983

2. Correlation-Based Method (CBM), which uses a correlation-based technique[13, 14]. In this case, the user defines on the first image of the series (chosen as a template image) a rectangular ROI (Figure 1), the size of which are assumed larger than the marker' size and where to search for the marker position. Within the ROI, the user needs to select a sub-ROI (mask) circumscribing the marker. The mask scans the ROI in a pixel stepwise manner, calculating the correlation between the actual mask and the chosen one onto the template image. The actual mask position associated to the best correlation value is assumed being the winning position, i.e. the assumed position of the marker in the given image.After a controlled thermal stress – as it is usually performed in fIRI [8, 11, 12] - the marker can become warmer (colder) then the surrounding tissue and the correlation becomes negative, thus suggesting to taking into account the absolute correlation value.

The estimated actual positions of the markers provides the parameters for the transformation (1), where for each pixel X and Y are the coordinates in the non-correct image; X' and Y' are the coordinates in the correct image; b_1 and b_2 are the translation terms; α is the rotation angle; s is a coefficient of scale, not used if the rigid body is constrained on a plane parallel to the projection one.

$$\begin{aligned} X' &= s\cdot\left(\cos(\alpha)X - \sin(\alpha)Y\right) + b_1 \\ Y' &= s\cdot\left(\sin(\alpha)X + \cos(\alpha)Y\right) + b_2 \end{aligned} \qquad (1)$$

The correlation value is calculated by the following formula(2), where: T_{XY} and $T_{X'Y'}$ are the temperatures in the two images of correspondent pixels; N is the number of pixels in the mask; c is the correlation value:

$$c = \frac{N\sum T_{XY}T_{X'Y'} - \sum T_{XY}\sum T_{X'Y'}}{\sqrt{\left[N\sum T_{XY}{}^2 - \left(\sum T_{XY}\right)^2\right]\left[N\sum T_{X'Y'}{}^2 - \left(\sum T_{X'Y'}\right)^2\right]}} \qquad (2)$$

Then, according to Zitova [13], we have applied a bilinear interpolation to reduce artifacts onto the transformed images.

Reliability of MC methods can be "measured" through analysis of the associated errors:

- 'localization error' on marker, that is the displacement of the marker coordinates due to their inaccurate detection;
- 'matching error', that is a mismatch error that occurs when more than one marker is tracked at once. This error can't occur because we track one marker at a time;
- 'alignment error', that is the error due to imperfect correspondence of the mapping model to the actual distortion or to a non precisely detection of markers. A mechanical constraint can been used to permit subject's movement only within the projection plane, thus reducing this kind of error as much as possible.

- *Localization error* : to evaluate this kind of error committed by the two methods a comparison with human-selection method has been computed.

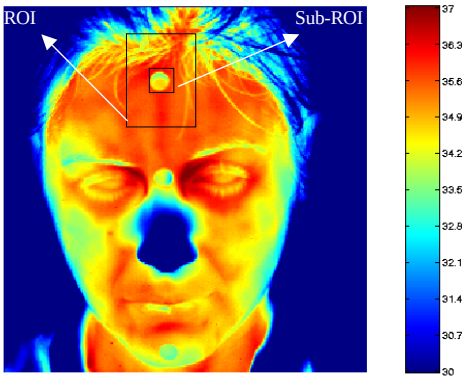

Figure 1: Template image with defined marker, sub-ROI (mask), and ROI.

Marker tracking based on CMM and CBM has been tested on three different 15 images-series [head (Fig. 2), chest (Fig. 3), and arm during a cold stress(Fig. 4); Test #1, #2, and #3, respectively] to assess methods' reliability in three different allowed conditions: little motion, large motion and large temperature variation. For each set, a given marker has been chosen on the template image. Then, the square Euclidean distance between the actual marker positions computed by CMM and CBM and the position selected by the human operator (i.e., the real position) has been computed on each image, and those distances averaged (3):

$$e = \frac{1}{N-1}\sum_{n=2}^{N}\left(\left(X_{auto}(n) - X_{human}(n)\right)^2 + \left(Y_{auto}(n) - Y_{human}(n)\right)^2\right) \qquad (3)$$

Where N is the total number of images of the series, $X_{auto}(n)$ and $Y_{auto}(n)$ are the coordinates found by the automatic method in n^{th} image, $X_{human}(n)$ and $Y_{human}(n)$ are the coordinates selected by the operator in the same image.

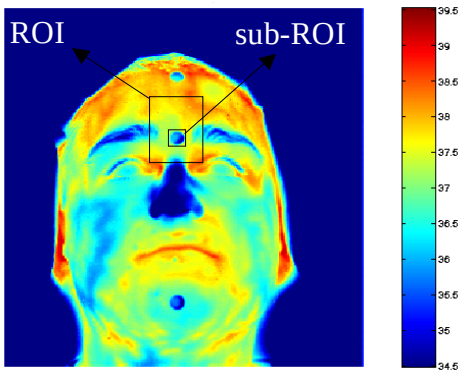

Figure 2: Image used in Test #1 performed on image series of face recorded while blocking the head (little motion allowed)

ISSN: 1727-1983

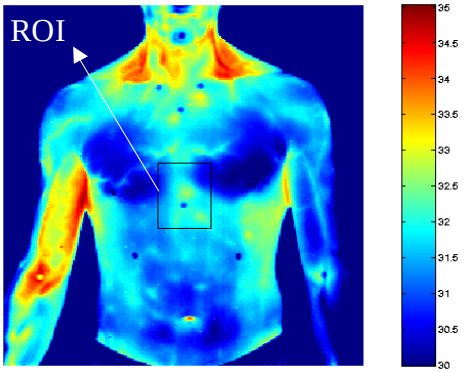

Figure 3: Image used in Test #2 performed on image series of chest during an exercise (large motion allowed)
.

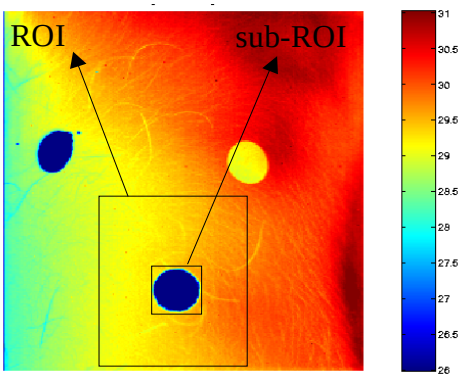

Figure 4: Image used in Test #3, while recording recovery from a cold stress (large temperature variation allowed).

- *Alignment error*: A Test Point Error (TPE) [13] to evaluate the 'alignment error' has been performed. It consisted of aligning a set of images using two markers and verifying method's consistency on a third different marker, manually tracked. The mean square of horizontal and vertical displacement of the test point has been calculated. The same test, on the same set of images, has been performed using a commercial fMRI data processing program to evaluate the effectiveness of the methods hereby proposed.

Methods' performance have been benchmarked correcting a series of 1278 images of the face by means of home-made software on an Athlon XP 2000+ processor and 512 Mb RAM running no other processes. The test has been repeated three times, and results average has been obtained.

Results

Results of tests are summarized in Tables 1, 2 and 3. Data are reported as mean ± SE.

Table 1: 'Localization error' test

	CMM Average Error (pixels)	**CBM Average Error (pixels)**
Test #1: Little motion allowed	2.1 ±0.3	0.5±0.3
Test#2: Large motion allowed	4.2 ±0.3	1.1 ±0.3
Test #3: Large temperature variation allowed	19.3±0.3	1.3±0.3

Table 2: Test Point Error

	Horizontal displacement Mean square Error (pixels^2)	**Vertical displacement Mean square Error (pixels^2)**
fMRI program	0.36±0.03	1.10±0.03
CMM	0.30±0.03	0.19±0.03
CBM	0.20±0.03	0.13±0.03

Table 3: Methods' performance

	CMM	**CBM**	**Human selection (estimated)**
Whole series average processing time **(seconds)**	30±1	69±1	3834 ± 1
Single image average processing time **(seconds)**	0.0235	0.054	3

Discussion

For what it concerns both 'localization' and 'alignment' error, CBM provides better results than CMM, in each of the test series. Particularly, CBM seems provide better performances while tracking markers' position during thermal stresses since it effectively tracks markers even in presence of large temperature variations.

In addition, since CBM stores the correlation values of the best estimated matching sub-ROY for each image of the set, an after-computation judgment of the

ISSN: 1727-1983

tracking effectiveness is possible. In fact, low correlation values expresses the impossibility of finding the template pattern in the actual ROI.

Both CMM and CBM seem working better than the tested non-fIRI MC method, according to the results of the TPE.

Time needed to process data by human selection based MC resulted roughly 3 seconds per image while performing 'localization error' test. Such a time is much more longer than the time requested by CMM and CBM to perform the same action.

CBM is slower than CMM, requesting twice time than the latter one.

Conclusions

Both proposed methods for MC of fIRI image series seem to provide suitable tools for data processing. They also seem giving better results than not-dedicated fIRI programs.

The CBM provides a better MC; it can be applied in a wider range of paradigms, but it requires longer computation time.

Furthermore the CBM can be used to track extended objects or large regions of interest. Such a method might be also implemented to perform feature-based tracking and MC, thus avoiding use of paper markers. For example, it might be implemented to automatically track and correct the position of given regions with specific anatomical features (nose, periorbital region, knee).

Further developments of the proposed methods should contemplate better interpolation algorithms. The proposed methods rely on the assumption of rigid body motion. Of course, this is an assumption valid in a limited range of situations. Therefore, advanced deformation models need to be developed for a more general application. To the best of our knowledge, this is the first attempt to develop dedicated MC automatic algorithms which can improve reliability and processing time for fIRI image series.

References

[1] ASHBURNER J., FRISTON K. (1997): 'Spatial transformation of images', *Human Brain Function*, pp. 43-58

[2] GIACHETTI A. (2000): 'Matching techniques to compute image motion', *Image Vision Comput 2000*, **18**, pp. 247–260

[3] COLLIGNON, A., MAES, F., DELAERE, D., VANDERMEULEN, D., SUETENS, P., AND MARCHAL (1995): 'Auto-mated Multi-Modality Image Registration Based on Information Theory', *Information Processing in Medical Imaging*, pp 263-274

[4] WOODS, R. P., CHERRY, S. R., MAZZIOTTA (1992): 'Rapid automated algorithm for aligning and reslicing PET images', *J. Comput. Assist. Tomogr.*, **16**, pp. 620-633

[5] GARBEY M., MERLA A., et al. (2004): 'Estimation of Blood Flow Rate and Vessel Location through Thermal Video', *IEEE Computer Society Conference on Computer Vision and Pattern Recognition*

[6] GARBEY M., MERLA A., et al. (2005):'Imaging the Cardiovascular pulse', *IEEE Computer Society Conference on Computer Vision and Pattern Recognition*

[7] MERLA A. (2004): 'Functional Infrared Imaging in Clinical Applications, Medical Infrared Imaging Workshop', proceeding on EMBS 2004 - Engineering in Medicine and Biology Society Conference, San Francisco, CA, , 2004.

[8] MERLA A., DONATO LD., et al. (2002): 'Quantifying the Relevance and Stage of Disease with the Tau image Technique', *IEEE Engineering in Medicine and Biology*, **21**, pp. 86 - 91

[9] MERLA A., DONATO LD., AND ROMANI G. (2002): 'Infrared Functional Imaging: Analysis of skin temperature during exercise', proceeding on EMBC 2002 - XXIV IEEE Engineering in Medicine and Biology Society Conference, Houston, TX, USA, 2002.

[10] MERLA A., ROMANI GL. (2005):'Biomedical Applications of Functional Infrared Imaging', proceeding on EMBC 2005 - Engineering in Medicine and Biology Society Conference, Shanghai, China, 2005.

[11] MERLA A., DI DONATO L., SALSANO F., ROMANI GL. et al. (2002): 'Raynaud's Phenomenon: infrared functional imaging applied to diagnosis and drugs effects', *International Journal of Immunopathology and Pharmacology*, **15**, no.1, pp. 41-52

[12] MERLA A., SALSANO F., ROMANI GL et al. (2002): 'Infrared Functional Imaging Applied to Raynaud's Phenomenon', *IEEE Engineering in Medicine and Biology Magazine*, **21**, N. 6, pp. 73 – 79

[13] ZITOVA B. , FLUSSER J. (2003) : ' Image registration methods: a survey', *Image and Vision Computing*, **21**, pp- 977-1000

[14] PRATT W.K. (1991): 'Digital Image Processing', (J. Wiley and Sons, New York)

ISSN: 1727-1983